

# Myosin Va facilitates the distribution of secretory granules in the F-actin rich cortex of PC12 cells

Rüdiger Rudolf<sup>1</sup>, Tanja Kögel<sup>1</sup>, Sergei A. Kuznetsov<sup>1,\*</sup>, Thorsten Salm<sup>1</sup>, Oliver Schlicker<sup>1</sup>, Andrea Hellwig<sup>1</sup>, John A. Hammer III<sup>2</sup> and Hans-Hermann Gerdes<sup>1,‡</sup>

<sup>1</sup>Department of Neurobiology, Interdisciplinary Center of Neuroscience, University of Heidelberg, Im Neuenheimer Feld 364, D-69120 Heidelberg, Germany

<sup>2</sup>Laboratory of Cell Biology, National Heart, Lung and Blood Institute, National Institutes of Health, Bethesda, MD 20892, USA

\*Present address: Institute of Cell Biology and Biosystems Technology, University of Rostock, Albert-Einstein Str. 3, D-18051 Rostock, Germany

‡Author for correspondence (e-mail: hhgerdes@uni-hd.de)

Accepted 12 December 2002

Journal of Cell Science 116, 1339-1348 © 2003 The Company of Biologists Ltd  
doi:10.1242/jcs.00317

## Summary

Neuroendocrine secretory granules, the storage organelles for neuropeptides and hormones, are formed at the trans-Golgi network, stored inside the cell and exocytosed upon stimulation. Previously, we have reported that newly formed secretory granules of PC12 cells are transported in a microtubule-dependent manner from the trans-Golgi network to the F-actin-rich cell cortex, where they undergo short directed movements and exhibit a homogeneous distribution. Here we provide morphological and biochemical evidence that myosin Va is associated with secretory granules. Expression of a dominant-negative tail domain of myosin Va in PC12 cells led to an extensive clustering of secretory granules close to the cell periphery,

a loss of their cortical restriction and a strong reduction in their motility in the actin cortex. Based on this data we propose a model that implies a dual transport system for secretory granules: after microtubule-dependent delivery to the cell periphery, secretory granules exhibit a myosin Va-dependent transport leading to their restriction and even dispersal in the F-actin-rich cortex of PC12 cells.

Movie available online

Key words: Secretory granules, Myosin Va, hCgB-GFP, Cell cortex, F-actin, Organelle transport

## Introduction

Neuroendocrine secretory granules (SGs) are organelles that store neuropeptides and hormones and release their content by a depolarisation-induced, Ca<sup>2+</sup>-dependent fusion with the plasma membrane (PM) (Kelly, 1993). Recently, GFP fusion proteins specifically targeted to SGs were employed to analyse different aspects of SG motility in living cells, such as transport in neurites (Kaether et al., 1997; Lochner et al., 1998; Gerdes and Rudolf, 1999) or exocytosis (Burke et al., 1997; Lang et al., 1997). Detailed studies of the motility of SGs in the F-actin-rich vicinity of the PM revealed that a few percent of all GFP-labelled SGs display short periods of directed movement (Lang et al., 2000). By using a specific GFP mutant, it was possible to follow the transport of SGs directly after their biogenesis at the trans-Golgi network (TGN) (Rudolf et al., 2001). This study showed that the delivery of SGs from the TGN to the cortical area occurred within a few seconds via microtubule (MT)-dependent transport (Rudolf et al., 2001) and that at any time-point about 70-80% of SGs were located in the subplasmalemmal region (Rudolf et al., 2001). Since this region is known to be rich in F-actin while MTs do not extend substantially into this area (Nakata and Hirokawa, 1992), it is likely that transport of SGs in the F-actin-rich cortex is accomplished via myosin motors along actin filaments. Prime candidates for such transport are class V myosin motors (Mermall et al., 1998). Myosin V is composed of two heavy chains which dimerise via a coiled-coil motif located in the stalk

region of the heavy chain (Cheney et al., 1993). The heavy chains contain an N-terminal, actin-binding motor domain (Cheney et al., 1993) followed by a neck region to which up to six regulatory light chains are bound, and a C-terminal globular domain (Cheney et al., 1993) which is thought to mediate organelle binding specificity (Reck-Peterson et al., 2000). To date, different subtypes of myosin V have been described in higher vertebrates (Reck-Peterson et al., 2000). The isoform most thoroughly investigated is myosin Va which has been shown to be associated with different organelles like small synaptic vesicles (Prekeris and Terrian, 1997) and melanosomes (Wu et al., 1997; Rogers and Gelfand, 1998). To assess the role of myosin Va in melanosome trafficking, *dilute* mice lacking functional myosin Va serve as a model system (Mercer et al., 1991). These mice exhibit a dilute fur colour and a lethal neuropathological phenotype (Mercer et al., 1991). While the underlying cause for the neurological phenotype is still a matter of debate, the pigmentation defect was found to originate from a mislocalisation of the pigment-containing melanosomes in melanocytes. In wild type melanocytes these melanosomes are captured in the cell cortex by the action of myosin Va, whereas in *dilute* melanocytes they display a loss of cortical localisation and an extensive clustering near the cell center (Wu et al., 1998). In addition to a change in subcellular distribution, short directed movements of melanosomes in the cell cortex observed in MT-depleted wild type melanocytes, were absent in melanocytes of *dilute* mice (Wu et al., 1998).

Because these two features of myosin Va-dependent melanosome transport, the restriction in the actin-cortex (Wu et al., 1998) and the execution of short, directed movements in the same area (Wu et al., 1998), were also found for SGs in PC12 cells (Rudolf et al., 2001), we tested whether myosin Va is involved in the subcellular distribution and motility of SGs. For this purpose we took advantage of a recently developed GFP-based pulse/chase-like system which permits the observation of SGs as they move from their site of synthesis, the TGN, to their site of storage, the subplasmalemmal region (Rudolf et al., 2001). Notably, with this system the features of SG transport and the underlying molecular mechanisms can be addressed with high spatial-temporal resolution. Using this method in combination with biochemical approaches, we here show that SGs undergo myosin Va-based transport in the F-actin rich cortex. Expression of a dominant negative mutant of myosin Va results in a strong reduction in SG motility and in clustering of SGs close to the cell periphery.

## Materials and Methods

### Chemicals, antibodies and expression vectors

Monoclonal antibodies clone 2F7.1B1 against rat TGN38 and clone 219.6 against rat CgB were kindly provided by G. Banting (University of Bristol, UK) and W. B. Huttner (MPI for Molecular Cell Biology and Genetics, Dresden, Germany), respectively. Polyclonal antibody 718 against rat SgII is described elsewhere (Krömer et al., 1998). Polyclonal antibodies DIL1, DIL2 and HAM5 against myosin Va are raised against GST-fusion proteins (Wu et al., 1997). Secondary antibodies goat anti-rabbit-rhodamine, goat anti-mouse-rhodamine redX, goat anti-rabbit-HRP and goat anti-mouse-HRP were purchased from Jackson Immuno Research Labs (West Grove, PA). Expression construct pcDNA3/hCgB-GFP(S65T) was generated by restriction of pCDM8/hCgB-GFP(S65T) (Kaether and Gerdes, 1995) with *Hind*III and *Eco*RI and ligation of the obtained hCgB-GFP(S65T) cDNA fragment into pcDNA3 expression vector (Invitrogen, San Diego, CA) opened with the corresponding restriction enzymes. The expression vectors pCMV2/FLAG and pCMV2/FLAG-MCLT are described elsewhere (Wu et al., 1998) and plasmid pcDNA3/PTS1-GFP for labelling of peroxisomes was kindly provided by W. Just (University of Heidelberg, Germany).

### Cell culture and transfection

PC12 cells (rat pheochromocytoma cells, clone 251) (Heumann et al., 1983) were grown in DMEM supplemented with 10% horse serum and 5% fetal calf serum at 37°C and 10% CO<sub>2</sub>. Cells were transfected as previously described (Kaether et al., 1997) using a BioRad Gene Pulser (BioRad Laboratories, Hercules, CA). Expression of the transgene was increased by incubation with 10 mM sodium butyrate for 17.5 hours. For microscopic analysis transfected PC12 cells were plated on poly-L-lysine (PLL, 0.1 mg/ml, Sigma Chemical Co.) coated LabTek chambered 4-well coverglasses (Nalge Nunc Int., Naperville, IL) or 9 mm coverslips. For biochemical experiments, cells were plated on PLL-coated 100- or 150 mm diameter dishes.

### Preparation of secretory granules and subcellular fractionation

SGs were prepared in HBS buffer (10 mM Hepes/KOH/pH 7.2, 0.25 M sucrose, 1.6 mM Na<sub>2</sub>SO<sub>4</sub>, 1 mM Mg(Ac)<sub>2</sub>, 1 mM EDTA, and protease inhibitor cocktail), following a protocol described by Ohashi and Huttner (Ohashi and Huttner, 1994), which was slightly modified. In brief, a post-nuclear supernatant (PNS) was prepared and centrifuged for 10 minutes at 14,000 *g* (Beckman rotor TLA55) to remove the TGN. The resulting supernatant was loaded onto a step

gradient, consisting of a 30  $\mu$ l 2M sucrose cushion and 200  $\mu$ l 0.5 M sucrose, and was spun for 20 minutes at 137,000 *g* (Beckman rotor TLS55) to sediment SGs. Thereafter the fraction enriched in SGs was collected at the interface of the two sucrose solutions and subjected to equilibrium sucrose density gradient centrifugation according to a standard procedure (Tooze et al., 1991) except that a linear gradient from 0.8-2 M sucrose was used. Aliquots of gradient fractions and the cell homogenate were subjected to SDS-PAGE followed by western blotting as described (Kaether et al., 1997).

### Immunoisolation of secretory granules

A PNS of PC12 cells was centrifuged at 14,000 *g* for 10 minutes (TLA55). The obtained supernatant was spun at 100,000 *g* for 20 minutes (TLA55). The pellet was resuspended in HBS buffer and aliquots were incubated with DIL2 antibody for 4 hours at 4°C in HBS supplemented with 5% fetal calf serum (HBSS). Thereafter the suspensions were spun at 100,000 *g* for 20 minutes (TLA55) and the pellet was resuspended in HBSS. Then, magnetic beads (M-500 subcellular, Dynal ASA, Oslo, Norway), covalently coated with goat anti-rabbit IgG (Fc-domain) and resuspended in HBSS, were added and incubated under slow rotation for 2 hours at 4°C in a final volume of 1 ml. Thereafter, the membranes bound to the beads were isolated and washed 3 $\times$ 15 minutes in HBSS. The unbound membrane fraction was obtained by centrifugation for 20 minutes at 100,000 *g* (TLA55). The proteins of both fractions were analysed by western blotting using the 718 antibody against rat SgII.

### Electron microscopy

For immunoelectron microscopy, SGs from a TGN-depleted PNS (see above) were sedimented on PLL-coated coverslips placed at the bottom of a TLS 55 rotor tube levelled with plasticine. After centrifugation, the coverslips were carefully removed from the tube and fixed. For immunolabelling, the samples were first incubated with DIL2 antibody and then with protein A coupled to 10 nm gold particles according to the standard indirect immunofluorescence labelling protocol. Immunolabelled SGs or membrane pellets of sucrose equilibrium gradients fractions, obtained after dilution to 0.5 M sucrose and subsequent centrifugation at 100,000 *g* for 30 minutes (TLA55), were prepared for electron microscopic analysis as follows. The samples were fixed with 2% glutaraldehyde in 0.1 M sodium cacodylate, and after postfixation with reduced osmium the preparations were dehydrated and embedded in 'Epon' according to standard procedures. Electron micrographs were taken with a Zeiss EM 10 CR electron microscope.

For quantitative immunoelectron microscopy, random images were taken showing cross-sections of the sample from top to bottom. Image positives were digitised using an AGFA Argus II scanner at a resolution of 1200 dpi and visually inspected to determine the number of gold particles associated with SGs. Gold particles were counted as associated with SGs if their distance to the membrane of SGs was less than 25 nm and their distance to other membranes was more than 25 nm.

### GFP-labelling of organelles and indirect immunofluorescence analysis

To label SGs with GFP, PC12 cells were treated similarly as previously described (Rudolf et al., 2001). The cells were either transfected with pcDNA3/hCgB-GFP(S65T) or double transfected with pcDNA3/hCgB-GFP(S65T) and pCMV2/FLAG or pCMV2/FLAG-MCLT, respectively. To label peroxisomes, the cells were transfected with the plasmids PTS1-GFP and FLAG or FLAG-MCLT. The culture medium was replaced by block buffer (PBS supplemented with 1 mM CaCl<sub>2</sub> and 0.5 mM MgCl<sub>2</sub>) and the cells were incubated for 2 hours at 20°C. To release the temperature block, the block buffer

was replaced by culture medium pre-warmed at 37°C and the cells were incubated for different chase times at 37°C as indicated. Indirect immunofluorescence labelling of cells was performed as previously described (Kaether et al., 1997). F-actin was fluorescently labelled with a phalloidin-TRITC conjugate (250 nM final concentration). Prior to analysis the cells were incubated for 2 hours at 20°C and then for 90 minutes at 37°C.

#### Qualitative and quantitative fluorescence analysis

Images for qualitative and quantitative colocalisation analysis were taken with a Leica TCS 4D confocal microscope (resolution of 512×512 pixels) equipped with an Ar/Kr laser, a 488/568 nm beamsplitter, 525/50 nm bandpass and 590 nm longpass emission filters, and a 63×/1.4 NA PL APO objective lens. Image analysis was

performed as previously described (Rudolf et al., 2001). Images for the colocalisation analysis of single granules sedimented on coverslips were taken with a Leica SP2 confocal microscope equipped with an Ar-laser (488 nm line), a He/Ne-laser (543 nm line), a 488/543/633 nm tripel-pass beamsplitter, emission detector sliders set to 493–527 nm (GFP-signal) and 581–666 nm (rhodamine-signal) opening and a 63×/1.4 NA PL APO objective lens. To maximise spatial resolution and signal-to-noise ratio, images were taken at a resolution of 1024×1024 pixels and 16× line averaging and then transferred to IPLab 3.2.2 software (Scanalytics, Fairfax, VA). Quantification of colocalisation between GFP-fluorescent SGs and the corresponding immuno-signals was performed as described (Kaether et al., 1997). Signals were scored as colocalising when their signal intensity maxima matched within a circle of 150 nm diameter.

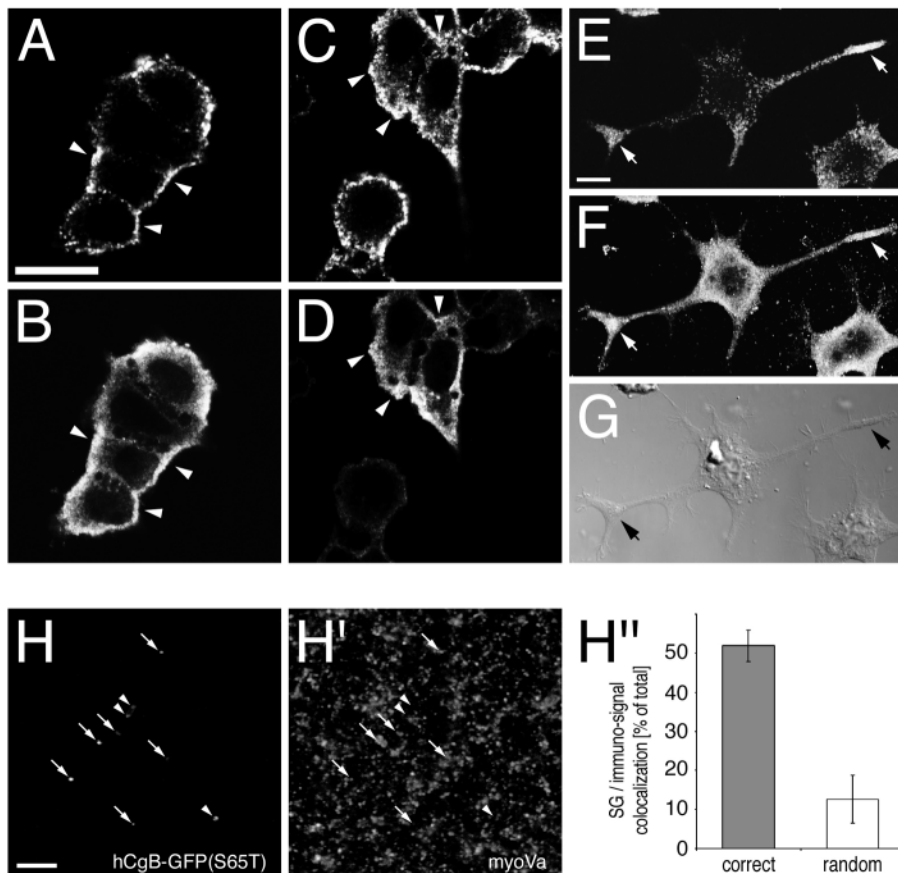


**Fig. 1.** Myosin Va is distributed in the cortex of PC12 cells and colocalises with rCgB. (A–G) Non-transfected PC12 cells were cultured for 2 days in the absence (A–D) or presence (E–G) of NGF. Then, the cells were fixed and immunostained against rCgB (B,D,F) and myosin Va with DIL1 (A) and DIL2 (C,E) antibody, respectively. Single corresponding confocal sections (AB, CD, EF) are shown. G shows a Nomarski image of the same cells as in E and F. Arrowheads in A–D, show cortical subdomains enriched in both rCgB and myosin Va; arrows in E–G indicate growth cones. Bars, 10  $\mu$ m. (H–H'') Cells were transfected with hCgB-GFP(S65T). After incubation of cells for 2 hours at 20°C and then for 180 minutes at 37°C, a PNS was prepared and SGs were sedimented on coverslips by differential centrifugation, fixed, and immunostained with DIL2 antibody against myosin Va. Subsequently, single confocal sections of GFP-fluorescent SGs (H) and the corresponding immunosignals (H') were recorded. Arrows indicate immuno-positive, and arrowheads immuno-negative, GFP-fluorescent SGs (compare H and H'). Bar, 1  $\mu$ m. The colocalisation of fluorescent SGs with myosin Va was quantified (H''). Black bar, colocalisation of GFP-fluorescence and immuno-signals form corresponding frame pairs (correct); white bar, random colocalisation of GFP- and immuno-signals from non-corresponding frame pairs (random). Error bars, s.e.m. ( $n=20$  images, each 60×60  $\mu$ m) corresponding to >500 fluorescent SGs.

#### Live cell imaging and image analysis

Transfected cells grown on PLL-coated LabTek chambers (Nalge Nunc Int.) were imaged with a conventional Leica DM IRB microscope equipped with a 100 W mercury arc lamp, a HQ EGFP-filter set (AHF GmbH, Tübingen, Germany), a 100×/1.4 NA PL APO objective lens and a Photometrics Quantix II cooled CCD camera (Roper Scientific, Munich, Germany). Videos consisting of 20 frames were taken with 0.5 seconds exposure time at a frame rate of 1.3 Hz. Automated image analysis and determination of mean velocities was performed using the TillVISION software v3.3 (Till Photonics GmbH, Martinsried, Germany). The unspecific error of the automated quantification method was assessed by the analysis of fluorescent SGs in fixed cells resulting in an apparent mean velocity of about 0.1  $\mu$ m/second which was subtracted from the measured values (Fig. 5A).

## Results

### Myosin Va is associated with secretory granules

SGs of neuroendocrine PC12 cells undergo short directed (non Brownian) movements in the F-actin-rich cell cortex (Rudolf et al., 2001). To address whether this movement reflects active, F-actin-dependent transport via myosin motors, we investigated the presence of unconventional myosin Va on SGs. Using double-immunofluorescence microscopy, we initially analysed if myosin Va is co-distributed with SGs. In non-differentiated PC12 cells, myosin Va stained with two different antibodies (Fig. 1A,C) was mainly localised in the cell periphery, like chromogranin B (CgB) (Huttner et al., 1991), a marker protein for SGs (Fig. 1B,D). Both proteins were localised in certain peripheral subdomains (Fig. 1A–D,

arrowheads) although myosin Va was more evenly distributed in the cortical area as compared to CgB. In PC12 cells differentiated with nerve growth factor, myosin Va showed a strong signal in the growth cones of neurites (Fig. 1E, arrows) where SGs were also highly concentrated (Fig. 1F, arrows). To analyse the significance of the observed colocalisation of both proteins in the cortical area, we circumvented the limitations in spatial resolution *in situ* by analysing the colocalisation of myosin Va and green fluorescent SGs *in vitro*. SGs were labelled with GFP in a pulse/chase-like manner by exploiting the temperature-sensitive folding mutant hCgB-GFP(S65T) (Rudolf et al., 2001) resulting in a small fluorescent subset (about 1%) of the total cellular SGs. This simplifies a quantitative analysis of the colocalisation, and additionally, constitutes a pool of SGs with a defined maturation status thus permitting a direct comparison of these data with those obtained from other experiments (see below). SGs, isolated from cells by subcellular fractionation, were spun on a coverslip, fixed and immunostained for myosin Va (Fig. 1H,H'). The number of GFP fluorescence signals indicating fluorescent SGs (panel H) was much less compared to the number of immunofluorescence signals indicating myosin Va positive structures (Fig. 1H'). Analysis of 692 green fluorescent SGs revealed  $52\pm 4\%$  (s.d.,  $n=38$  fields) colocalisation with immunofluorescence signals of myosin Va (Fig. 1H'). As a control for specific colocalisation, we determined the random colocalisation by analysing non-corresponding frame pairs of GFP- and immunofluorescence. This resulted in an apparent colocalisation value of  $13\pm 6\%$  (s.d.,  $n=10$  fields). Thus, a significant colocalisation between SGs and myosin Va was evident. The non-colocalising granules may represent a second pool of these organelles possessing very little or no myosin Va.

To resolve the association of myosin Va with SGs at the ultrastructural level, we performed electron microscopy of immunolabelled membrane structures. SGs were sedimented by ultracentrifugation from a TGN-depleted PNS on

coverslips and then processed for immunoelectron microscopy. Staining with a myosin Va-specific antibody resulted in a peripheral immunogold labelling of dense-core structures (Fig. 2B, exemplified by open arrowheads). Under control conditions, i.e. the presence of protein A-gold and the absence of myosin Va antibody, almost no labelling of dense-core structures was found (Fig. 2A, exemplified by arrowheads). A quantitative analysis revealed that the myosin Va immunolabelling was highly specific for SGs.  $45.8\pm 8.7\%$  (s.d.,  $n=1278$ ) of the analysed gold particles were located to SGs and  $41.5\pm 3.6\%$  (s.d.,  $n=478$ ) of all SGs were labelled on average with 3.5 gold particles per SG. In control experiments only  $2.8\pm 1.6\%$  (s.d.,  $n=347$ ) and  $7.9\pm 1.7\%$  (s.d.,  $n=441$ ) of immunogold labelled SGs were detected in the absence of myosin Va antibody or in the presence of myosin Va antibody preincubated with the antigen, respectively. This data strongly suggests that approximately half of SGs are associated with myosin Va.

To further corroborate that myosin Va is bound to SGs, we analysed whether the motor protein copurified with SGs *in vitro*. Therefore, SGs were enriched from a TGN-depleted PNS by differential centrifugation and subsequently loaded onto a sucrose density equilibrium gradient to separate the vesicular components according to their buoyant density. The obtained gradient fractions were analysed by western blotting to determine the distribution of myosin Va (Fig. 3A) and secretogranin II (SgII), a marker protein for SGs. This showed that the peak of myosin Va (Fig. 3B, fractions 9,10) coincides with the peak of SgII (Fig. 3B, fractions 9,10). Furthermore, the analysis of pelleted membranes of fraction 9 by electron microscopy revealed a high enrichment in dense-core SGs (Fig. 3C). Interestingly, SgII exhibited a second maximum in fractions 6-8 which contained approximately 40% less myosin Va as compared to the main peak. Since immature secretory granules represent only a few percent of total SGs under steady state conditions (Tooze et al., 1991) as used here, these fractions may reflect a different

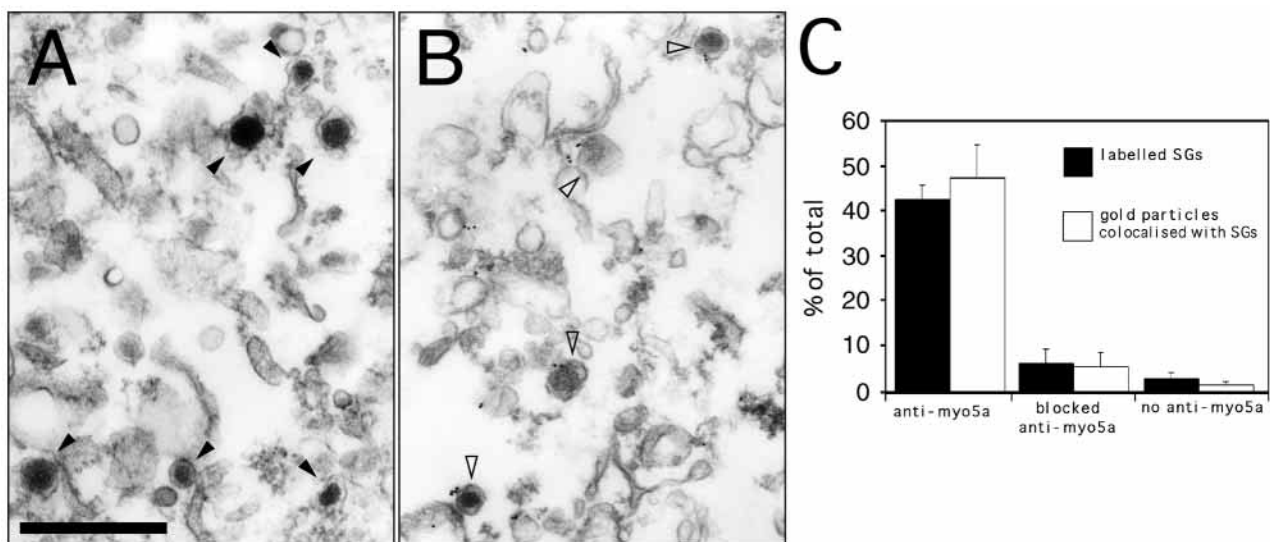


**Fig. 2.** Myosin Va is associated with SGs at the ultrastructural level. SGs from non-transfected PC12 cells were prepared by differential centrifugation (see Materials and Methods). SGs were then processed for immunoelectron microscopy in the absence (A) or presence (B) of anti-myosin Va, or with blocked anti-myosin Va (not shown), and protein A 10 nm immuno-gold (A,B). Bar, 500 nm. Unlabelled SGs (A, filled arrowheads) and labelled SGs (B, open arrowheads) are indicated. A quantification of the myosin Va immunolabelling of SGs is shown in C.

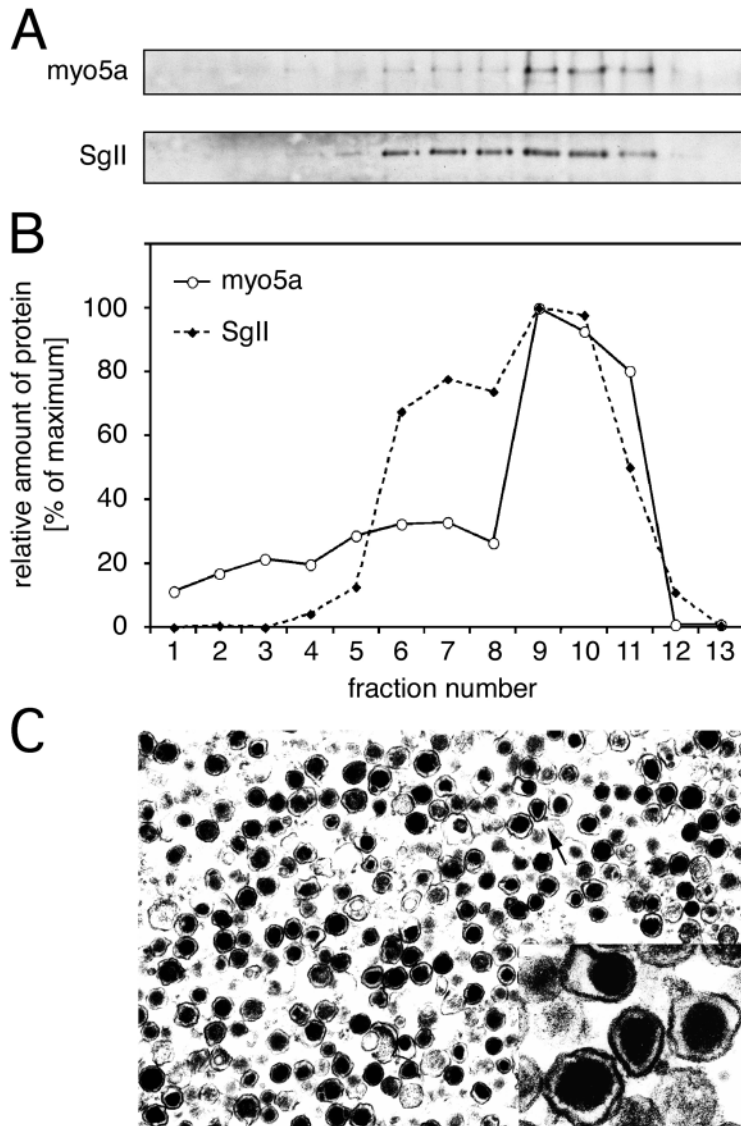


**Fig. 3.** Myosin Va cofractionates with SGs on sucrose gradients. A PNS of non-transfected PC12 cells was subjected to differential and then to equilibrium sucrose gradient (0.8–2 M sucrose) centrifugation. Equal aliquots of the final equilibrium gradient fractions (top, fraction 1) were analysed by western blotting for myosin Va and rSgII (A). The graph shows the intensity profiles of the two proteins (B). The membranes of fraction 9 of the gradient were pelleted, embedded in 'Epon' and analysed by electron microscopy (C). Bar, 500 nm. The arrow indicates the magnified area shown at the bottom right.

pool of secretory granules, e.g. small mature secretory granules of PC12 cells that have been documented by Huttner and colleagues (Bauerfeind et al., 1993). In conclusion, this biochemical data further support that myosin Va is present on SGs.

To further demonstrate the association of myosin Va with SGs, we employed immunoprecipitation of SGs using the DIL2 antibody against myosin Va. For this purpose, a fraction of a PC12 cell homogenate enriched in SGs, was prepared by differential centrifugation. This fraction was incubated with DIL2 antibody and subjected to immunoprecipitation using magnetic beads. Subsequently, the amount of SGs in the

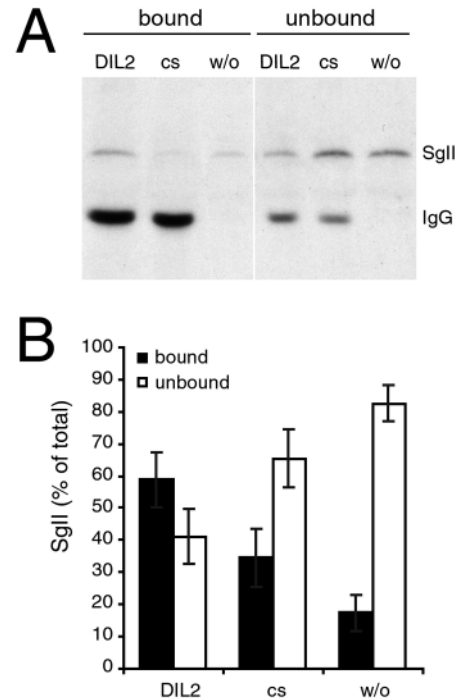


**Fig. 4.** Immunoprecipitation of SGs. (A) A PNS of PC12 cells was fractionated by differential centrifugation. The fraction enriched in SGs was incubated with myosin Va-specific serum (DIL2), control serum (cs) or without serum (w/o). The membranes bound to antibodies were isolated by immunoprecipitation with magnetic beads covalently coated with secondary antibodies. Bound (bound) and unbound membranes (unbound) were analysed by western blotting using antibodies against SgII. The signals for SgII (SgII) and the IgG heavy chain (IgG) are indicated. (B) The bar graph shows a quantitative analysis of seven independent experiments. For each experiment the sum of SgII in the respective unbound and bound fraction was set to 100%. Note that the differences between values obtained for the myosin Va serum and the controls are highly significant (paired *t*-test,  $P < 0.005$ ). Error bar, s.e.m.

respective bound and unbound fractions was determined by analysing the amount of SgII, a matrix protein of SGs. Fig. 4A depicts the western blot of a representative experiment including two controls. It shows that, in the case of the DIL2 antibody, the majority of SgII was detected in the bound fraction. Quantification revealed that  $58.9 \pm 8.6\%$  (s.e.m.,  $n=7$ ) of SgII was isolated with the DIL2 antibody,  $34.6 \pm 9.1\%$  (s.e.m.,  $n=7$ ) with the control antibody and  $17.5 \pm 5.7\%$  (s.e.m.,  $n=7$ ) in the absence of an antibody (Fig. 4B). This result shows that about one third to one half of SGs can be immunoprecipitated with the myosin Va antibody and suggests that, in conjunction with our immunofluorescence and immunoelectron microscopic data, a fraction of SGs is associated with myosin Va.

#### Expression of myosin Va tail fragment strongly reduces the motility of SGs

To test whether inhibition of the motor activity of myosin Va leads to a reduction in motility of SGs, we analysed the

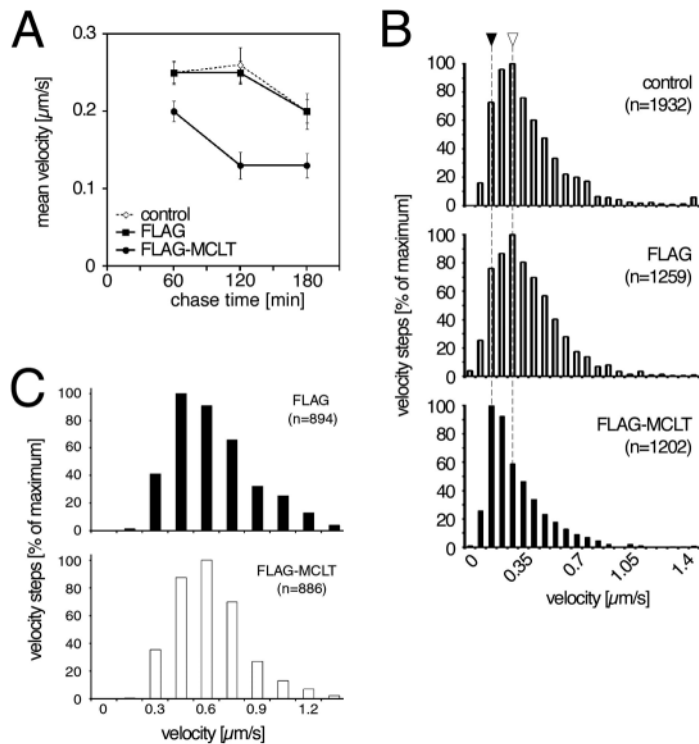


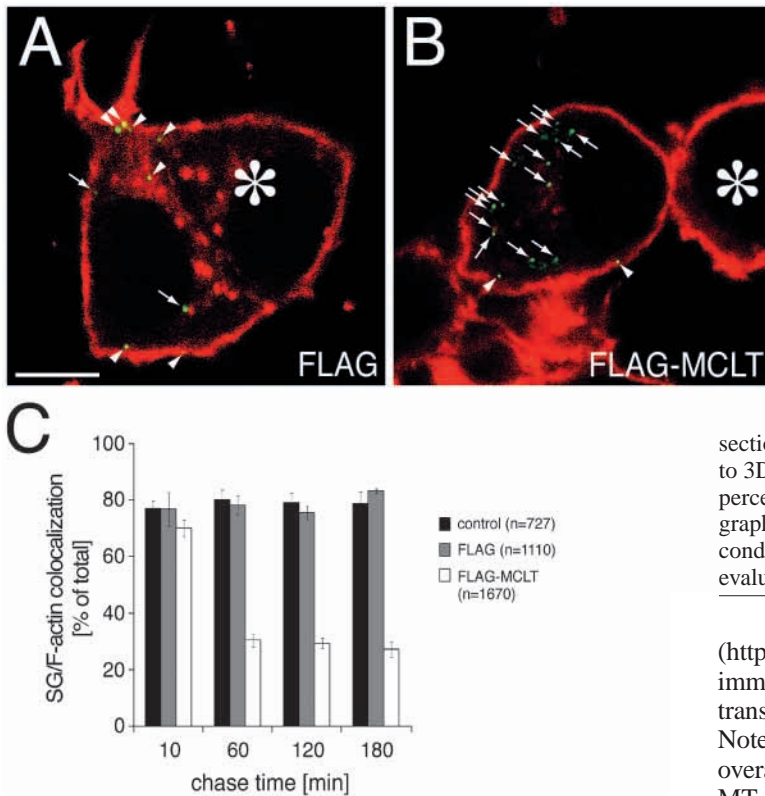
**Fig. 5.** Expression of FLAG-MCLT reduces the velocity of SGs. (A,B) PC12 cells, either single-transfected with hCgB-GFP(S65T) (control) or double-transfected with hCgB-GFP(S65T) and FLAG (FLAG) or FLAG-MCLT (FLAG-MCLT), respectively, were incubated for 2 hours at 20°C and then at 37°C as indicated. Cells were imaged at 37°C and the movements of SGs were tracked automatically. For each time point and condition at least 20 cells from four independent experiments were analysed. (A) Mean velocities of all SGs per cell are plotted as a function of chase time. Prior to plotting, the system-inherent error of the automated tracking algorithm used was subtracted from all values (see Materials and Methods). Error bars, s.e.m. (B) Frequency distributions of all velocity steps (n) recorded from frame to frame for each condition over the observation time indicated in A. Open arrowhead, maximal number of steps measured for control and FLAG-transfected cells; filled arrowhead, maximal number of steps measured for FLAG-MCLT-transfected cells. (C) PC12 cells, co-transfected with pcDNA3/PTS1-GFP and FLAG or FLAG-MCLT, respectively, were incubated for 2 hours at 20°C and then for 90 minutes at 37°C. Cells were imaged at 37°C and the movements of peroxisomes were tracked automatically. The frequency distributions of all velocity steps (n) are shown for each condition (C).

average velocity of SGs as a function of their age in the presence and absence of a C-terminal tail fragment of myosin Va, FLAG-MCLT. This tail fragment is known to act as a potent inhibitor of myosin Va function in mouse melanocytes (Wu et al., 1998). To generate a limited number of GFP-fluorescent SGs with a defined age, we exploited the GFP-based pulse/chase-like system (Rudolf et al., 2001). Cells were double-transfected with hCgB-GFP(S65T) and FLAG or FLAG-MCLT, respectively, incubated for 2 hours at 20°C and analysed using video microscopy after different chase times. Thereafter, the vesicle movements were automatically analysed by a computer algorithm (Tvaruskó et al., 1999) to determine the average velocities of green fluorescent SGs. While the co-expression of FLAG did not alter the motility of

SGs as compared to the single hCgB-GFP(S65T)-transfected cells (Fig. 5A), the presence of FLAG-MCLT led to a strong reduction in velocity (Fig. 5A). This reduction was most prominent after 2 hours of chase (Fig. 5A). To analyse which range of velocity was affected by FLAG-MCLT, the frequency distributions of the velocity steps from all SG tracks obtained under the respective conditions were calculated. Under control conditions (Fig. 5B, control, FLAG) the velocity steps displayed a broad distribution with a maximum at 0.28 μm/second (Fig. 5B, open arrowhead). In contrast, in the presence of FLAG-MCLT, the maximum was shifted to 0.14 μm/second (Fig. 5B, filled arrowhead). Furthermore, velocity steps in the range between 0.28 and 0.8 μm/second were less frequent. This range has been shown to be characteristic for myosin V-dependent transport in vitro (Cheney et al., 1993; Evans et al., 1998; Wang et al., 2000; Wang et al., 1996). To address the specificity of the FLAG-MCLT effect for granules, PC12 cells were double-transfected with the peroxisomal marker PST1-GFP and FLAG-MCLT. Notably, for peroxisomes we did not find a difference in the distribution of the velocity steps between FLAG- and FLAG-MCLT-transfected cells (Fig. 5C). This indicates that peroxisomes, known to undergo MT-dependent transport (Rapp et al., 1996), are not affected by the dominant negative tail of myosin Va. Together, these results strongly support a selective involvement of myosin Va in the cortical transport of SGs.

#### Expression of myosin Va tail fragment results in a loss of cortical restriction of SGs

To test whether myosin Va plays a role in capturing of SGs in the actin-rich cell cortex (Rudolf et al., 2001), we analysed the colocalisation of fluorescent SGs with cortical F-actin in the presence and absence of FLAG-MCLT as a function of chase time. Therefore, cells were single-transfected with hCgB-GFP(S65T) or co-transfected with hCgB-GFP(S65T) and FLAG or FLAG-MCLT, respectively. The cells were fixed after different chase times, F-actin was stained with phalloidin-TRITC and colocalisation was analysed as described (Rudolf et al., 2001). Fig. 6A,B shows single confocal sections of these preparations to illustrate the result for the 60 minute chase time point. In cells co-transfected with FLAG, the majority of SGs colocalised with F-actin (Fig. 6A, arrowheads). In contrast, the vast majority of SGs in cells co-transfected with FLAG-MCLT, was localised throughout the cytoplasm (Fig. 6B, arrows) and only a few were found in the cortical F-actin (Fig. 6B, arrowheads). A quantitative analysis revealed that in control cells, single-transfected with hCgB-GFP(S65T) or co-transfected with FLAG, 80% of fluorescent SGs were located in the cortical F-actin over the entire observation period (Fig. 6C) as has been shown previously (Rudolf et al., 2001). However, in the presence of FLAG-MCLT the cortical localisation of SGs was strongly reduced to about 30% between 60 and 180 minutes of chase (Fig. 6C). This suggests that myosin Va plays a role in capturing SGs in the F-actin-rich cell cortex. Interestingly, FLAG-MCLT did not affect the cortical capturing after 10 minutes of chase (Fig. 6C) which may indicate that



MT-dependent outward transport is unimpaired at this time-point.

### Expression of myosin Va tail fragment leads to clustering of SGs

Upon expression of the myosin Va tail fragment, SGs not only lost their cortical restriction but also appeared to accumulate in certain areas of the cells. This phenomenon was addressed by a thorough three-dimensional analysis. PC12 cells were co-transfected with hCgB-GFP(S65T) and FLAG or FLAG-MCLT, respectively, incubated for 2 hours at 20°C and then chased for 0 or 90 minutes at 37°C. After fixation, cells were immunostained against TGN38 and analysed by confocal double fluorescence microscopy. 40 optical sections were taken from each cell and rendered into three-dimensional representations (Fig. 7A-C'). Cells transfected with FLAG and fixed directly after the 20°C incubation period (0 minutes chase) showed a clustered, perinuclear green fluorescence signal which colocalised with the TGN38 immuno-signal (Fig. 7A,A'). The same signal pattern was observed for FLAG-MCLT under these conditions (not shown). When cells, co-transfected with FLAG, were chased for 90 minutes, the green fluorescence had left the TGN in SGs evenly distributed in the cell periphery (Fig. 7B,B') as previously reported (Rudolf et al., 2001). Also in the presence of FLAG-MCLT all GFP-fluorescent proteins had left the TGN after 90 minutes of chase (Fig. 7C,C'). However, in contrast to the control, SGs were not evenly distributed in the periphery of the cell, but were extensively clustered in a region between the TGN and the juxtaposed PM (Fig. 7C,C', arrowheads). A 3D view of this cell clearly shows that the SG clusters are located in the periphery of the cell [see supplementary 3D movie

**Fig. 6.** Expression of FLAG-MCLT inhibits the cortical localisation of SGs. PC12 cells were either single-transfected with hCgB-GFP(S65T) or double-transfected with hCgB-GFP(S65T) and FLAG or FLAG-MCLT, respectively, incubated for 2 hours at 20°C and then at 37°C as indicated. Cells were fixed, stained with phalloidin-TRITC for F-actin and then analysed by confocal double-fluorescence microscopy. For each cell, 40 optical sections were taken. (A,B) Overlays of single optical sections for hCgB-GFP(S65T) (green) and F-actin (red) from cells double-transfected with hCgB-GFP(S65T) and FLAG (A) or FLAG-MCLT (B), respectively, and fixed after 1 hour of chase. SGs colocalising with F-actin are indicated by arrowheads, non-colocalising SGs are indicated by arrows. Asterisks, nontransfected cells. Bar, 5  $\mu$ m. (C) Quantitation of colocalisation. The 40 optical

sections per colour channel were rendered with IPLab 3D-software to 3D representations (see Materials and Methods) and the percentage of SGs colocalising with F-actin was determined. The graph shows mean values for at least four cells per time point and condition from two independent experiments. n, number of SGs evaluated per condition. Error bars, s.e.m.

(<http://www.biologists.org/supplemental>]). Interestingly, also immunostained, rCgB-containing SGs in FLAG-MCLT single-transfected cells showed a clustered appearance (not shown). Noteworthy, the expression of FLAG-MCLT did not change the overall number of fluorescently labelled SGs per cell. Since fast MT-dependent outward transport of fluorescent SGs from the TGN was observed in the presence of FLAG-MCLT (not shown), it is likely that only the F-actin-dependent, cortical transport of SGs is severely affected by the presence of the tail fragment of myosin Va. Importantly, in contrast to SGs, coexpression of FLAG-MCLT did not induce cluster formation of GFP-labelled peroxisomes (Fig. 7F). This suggests that the expression of the tail fragment of myosin Va does not inhibit cellular membrane traffic in general but is selective for myosin Va associated organelles.

If FLAG-MCLT directly interacted with SGs, there should be an increased local concentration of FLAG-MCLT in the clusters of fluorescent SGs. This was investigated after 90 minutes of chase at 37°C under the same experimental conditions described above, followed by antibody staining against the FLAG-epitope of FLAG-MCLT. As anticipated, FLAG-MCLT showed a strongly clustered staining (Fig. 7D,E, arrowheads) colocalising with the accumulated green fluorescent SGs (Fig. 7D',E'), in addition to a diffuse cortical signal, best visible in single optical sections (Fig. 7D). In contrast, analysis of peroxisomes in double-transfected cells showed that FLAG-MCLT did not colocalise with GFP-labelled peroxisomes (Fig. 7F). This result is in accordance with the absence of peroxisome clusters. Together, our findings further support the idea that the tail fragment of myosin Va interacts specifically with SGs and interferes with their F-actin-dependent transport in the cortex.

## Discussion

### Recruitment and activity of myosin Va

We have provided strong morphological and biochemical evidence that in neuroendocrine PC12 cells the unconventional myosin Va is associated with at least half of all SGs per cell

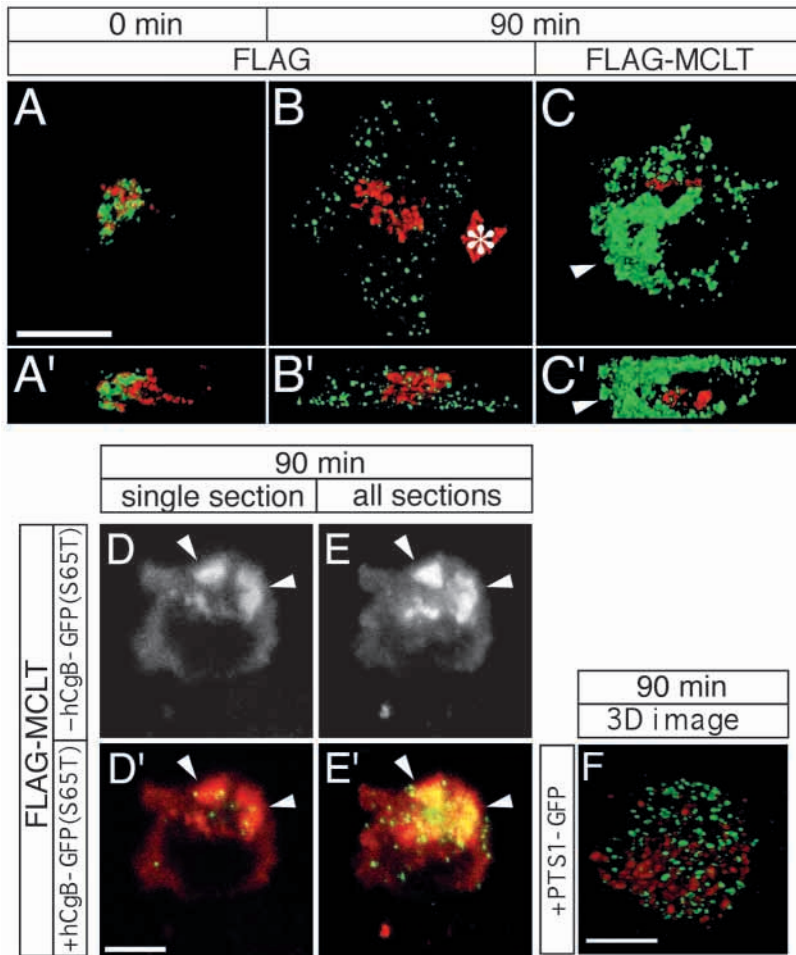


**Fig. 7.** Expression of FLAG-MCLT leads to clusters of SGs that colocalise with FLAG-MCLT. PC12 cells were double-transfected with hCgB-GFP(S65T) and FLAG (A-B' or FLAG-MCLT (C-E'), respectively, incubated for 2 hours at 20°C and then for 0 or 90 minutes at 37°C as indicated. Cells were fixed and immunostained against TGN38 (A-C') or the FLAG epitope (D-E'). For confocal double-fluorescence microscopy, 40 optical sections were taken for each cell. (A-C') Three-dimensional representations showing hCgB-GFP(S65T) in green and TGN38 immunostaining in red. The asterisk in B indicates the TGN of a non-transfected cell. (A-C) top views; (A'-C'), side views. Bar, 5  $\mu$ m. Note that in the presence of FLAG-MCLT SGs accumulate between the TGN and the juxtaposed PM. (D-E') Single confocal section through the center of the cell (D,D') or overlay of all 40 sections (E,E'). (D,E) FLAG-MCLT-immunostaining. (D',E') Overlay of hCgB-GFP(S65T) (green) and FLAG-MCLT-immunostaining (red). Colocalising signals are shown in yellow. (F) PC12 cells were co-transfected with PTS1-GFP and FLAG-MCLT, incubated for 2 hours at 20°C and then for 90 minutes at 37°C. Thereafter cells were fixed, immunostained against the FLAG epitope and analysed by confocal microscopy. A 3D image was rendered. Green, GFP-fluorescence, red, immunofluorescence. Bar, 5  $\mu$ m. See corresponding movie at <http://jcs.biologists.org/supplemental>.

and transports these storage organelles in the F-actin rich cortex. The existence of an additional granule pool, which is associated with much less or no myosin Va, remains a matter of speculation because we cannot exclude that the lack of signal was due to limitations of the experimental approach. We have found that upon expression, the dominant-negative tail fragment of myosin Va led to the clustering of SGs between the TGN and PM as well as to a reduction in their cortical

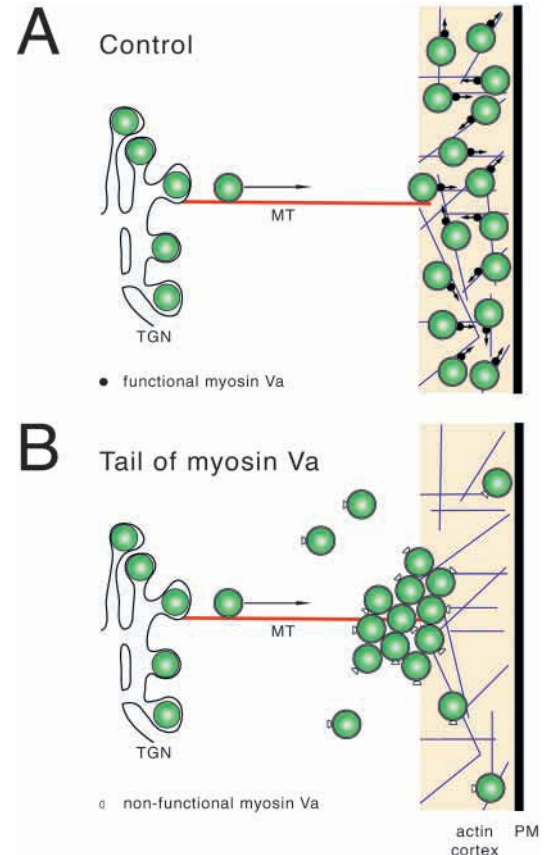


**Fig. 8.** The role of myosin Va in the transport of secretory granules. (A) After MT-dependent delivery from the TGN to the actin cortex, SGs (green spheres) are captured and removed from the cortical entry site by SG-bound active myosin Va (black circles) via transport along actin fibers as indicated by arrows. (B) The expression of the tail fragment of myosin Va (white semi-circles) blocks myosin Va-mediated capturing and transport of SGs in the actin cortex. This leads to a loss in cortical distribution and formation of clusters of SGs at the interface of the MT- and actin-networks.

localisation. These results together with the observed uni-directional transport of SGs from the TGN to the PM in undifferentiated PC12 cells (Rudolf et al., 2001) suggest that cluster formation in the presence of the tail fragment is due to a block of transport of SGs away from their site of MT-dependent delivery to the actin cortex (Fig. 8). According to this model clusters of SGs are formed at the interface between the MT-network and the actin cortex where network switching would occur (Fig. 8).

Both effects, cluster formation and a lack of cortical capturing, were also observed for melanosomes of melanocytes expressing the tail fragment of myosin Va as well as of melanocytes from *dilute* mice (Wu et al., 1998). However, the clusters of melanosomes were observed at the cell center and not in the cell periphery as was done with SGs. It is likely that this difference in the localisation of vesicle clusters is due to the bi-directional versus uni-directional MT-dependent

transport of melanosomes and SGs, respectively. Therefore it may be possible that melanosomes disabled to move along actin fibers undergo MT-dependent, centripetal transport leading to an accumulation in the region with the highest MT-density (Wu et al., 1998), whereas SGs, seemingly incapable of MT-dependent inward transport, accumulate at the cell periphery.

Upon expression of the tail fragment of myosin Va we observed in addition to clustered SGs a number of presumably single SGs which were distributed throughout the cytoplasm and not restricted to the cortex (Fig. 8). These SGs were strongly reduced in motility and showed no obvious MT-dependent movement (Fig. 8). In contrast, SGs from cells not co-transfected with the tail fragment but treated with latrunculin B to depolymerise F-actin, appeared to exhibit MT-dependent movement (Rudolf et al., 2001). This suggests that the association of SGs with the tail fragment may also negatively affect their MT-dependent transport.

### Existence and recruitment of motor protein complexes

The finding of actin-dependent transport of SGs together with previous observations showing an MT-dependent movement of newly formed SGs from the TGN to the PM (Rudolf et al., 2001) provides strong evidence for the existence of a dual transport system used by a secretory organelle (Fig. 8). Evidence for a dual transport system has also been found for melanosomes (Brown, 1999; Reck-Peterson et al., 2000), the endoplasmic reticulum (Tabb et al., 1998; Reck-Peterson et al., 2000) and phagosomes (Al-Haddad et al., 2001). Along these lines, it appears that motor proteins associated with the surface of organelles, are often organised in protein complexes (Schliwa, 1999). A direct interaction between microtubule- and actin-based transport motors has been shown for the ubiquitous kinesin heavy chain KhcU and myosin Va in mouse (Huang et al., 1999) as well as for the dynein light chain and myosin Va in chicken (Espindola et al., 2000). For SGs, MT-dependent motors have not been identified to date, but assuming that the direct interaction between MT- and actin-based transport motors is a general principle, myosin Va could be used as a tool to identify them.

Given that motor protein complexes exist on organelles, the intriguing question is, how these complexes are recruited and what mediates their membrane association. The first identified motor protein receptor was kinectin which is thought to mediate the binding of kinesin to membranes (Vallee and Sheetz, 1996; Ong et al., 2000). Recently, the C-terminal cytoplasmic tail of rhodopsin was found to facilitate the binding of dynein via the dynein light chain to rhodopsin-bearing vesicles (Tai et al., 1999). For myosin Va both the motor and the tail domain are thought to function in cargo binding (Evans et al., 1998). However, little is known about the putative interaction of these domains with cargo surface molecules. For small synaptic vesicles, it has been reported that the cytoplasmic domain of the synaptobrevin-synaptophysin complex may function as a binding partner for myosin Va (Prekeris and Terrian, 1997). Recently, a member of the small monomeric G-protein family rab, rab27a, has been implicated in the interplay between melanosomes and myosin Va (Deacon and Gelfand, 2001) and is now postulated to act as a 'receptor' for myosin Va (Wu et al., 2001).

Since different rab proteins show binding specificity for distinct organelles and play a role in the regulation of membrane traffic, it is likely that other members of the rab protein family may function in a manner similar to that of rab27a. Because rab3a is known to be specifically associated with small synaptic vesicles and SGs (Fischer von Mollard et al., 1990; Darchen et al., 1995), it is intriguing to speculate that this small GTP-binding protein may have a role in recruitment of myosin Va to SGs. In light of a recent study on PC12 cells by Martelli and colleagues our data strongly support this idea. They showed that the overexpression of a rab3a mutant protein deficient in GTP hydrolysis led to a decrease in the total number of SGs in the vicinity of the PM (Martelli et al., 2000). This is in agreement with our finding of a reduction in cortical localisation in the presence of the tail fragment of myosin Va. However, further studies will be necessary to test this hypothesis.

We thank George Banting for providing TGN38 antibody and Wieland B. Huttner for providing rCgB antibody. We thank Amin Rustom and Mark Bajohrs for critical comments on the manuscript. R.R. was supported by the Studienstiftung des deutschen Volkes and T.S. by Graduiertenstipendium des Landes Baden-Württemberg. H.-H.G. was a recipient of a grant of the DFG (GE 550/3-1) and Fonds der chemischen Industrie.

### References

- Al-Haddad, A., Shonn, M. A., Redlich, B., Blocker, A., Burkhardt, J. K., Yu, H., Hammer, J. A., 3rd, Weiss, D. G., Steffen, W., Griffiths, G. and Kuznetsov, S. A. (2001). Myosin Va bound to phagosomes binds to F-actin and delays microtubule-dependent motility. *Mol. Biol. Cell* **12**, 2742-2755.
- Bauerfeind, R., Régnier-Vigouroux, A., Flatmark, T. and Huttner, W. B. (1993). Selective storage of acetylcholine, but not catecholamines, in neuroendocrine synaptic-like microvesicles of early endosomal origin. *Neuron* **11**, 105-121.
- Brown, S. S. (1999). Cooperation between microtubule- and actin-based motor proteins. *Annu. Rev. Cell Dev. Biol.* **15**, 63-80.
- Burke, N. V., Han, W., Li, D., Takimoto, K., Watkins, S. C. and Levitan, E. S. (1997). Neuronal peptide release is limited by secretory granule mobility. *Neuron* **19**, 1095-1102.
- Cheney, R. E., O'Shea, M. K., Heuser, J. E., Coelho, M. V., Wolenski, J. S., Espreafico, E. M., Forscher, P., Larson, R. E. and Mooseker, M. S. (1993). Brain myosin-V is a two-headed unconventional myosin with motor activity. *Cell* **75**, 13-23.
- Darchen, F., Senyshyn, J., Brondyk, W. H., Taatjes, D. J., Holz, R. W., Henry, J. P., Denizot, J. P. and Macara, I. G. (1995). The GTPase Rab3a is associated with large dense core vesicles in bovine chromaffin cells and rat PC12 cells. *J. Cell Sci.* **108**, 1639-1649.
- Deacon, S. W. and Gelfand, V. I. (2001). Of yeast, mice, and men: rab proteins and organelle transport. *J. Cell Biol.* **152**, F21-F24.
- Espindola, F. S., Suter, D. M., Partata, L. B., Cao, T., Wolenski, J. S., Cheney, R. E., King, S. M. and Mooseker, M. S. (2000). The light chain composition of chicken brain myosin-Va: calmodulin, myosin-II essential light chains, and 8-kDa dynein light chain/PIN. *Cell Motil. Cytoskeleton* **47**, 269-281.
- Evans, L. L., Lee, A. J., Bridgman, P. C. and Mooseker, M. S. (1998). Vesicle-associated brain myosin-V can be activated to catalyze actin-based transport. *J. Cell Sci.* **111**, 2055-2066.
- Fischer von Mollard, G., Mignery, G. A., Baumert, M., Perin, M. S., Hanson, T. J., Burger, P. M., Jahn, R. and Sudhof, T. C. (1990). Rab3 is a small GTP-binding protein exclusively localized to synaptic vesicles. *Proc. Natl. Acad. Sci. USA* **87**, 1988-1992.
- Gerdes, H.-H. and Rudolf, R. (1999). Green light for the secretory pathway. *Protoplasma* **209**, 1-8.
- Heumann, R., Kachel, V. and Thoenen, H. (1983). Relationship between NGF-mediated volume increase and "priming effect" in fast and slow reacting clones of PC12 pheochromocytoma cells. *Exp. Cell Res.* **145**, 179-190.
- Huang, J. D., Brady, S. T., Richards, B. W., Stenolen, D., Resau, J. H.,

- Copeland, N. G. and Jenkins, N. A. (1999). Direct interaction of microtubule- and actin-based transport motors. *Nature* **397**, 267-270.
- Huttner, W. B., Gerdes, H.-H. and Rosa, P. (1991). The granin (chromogranin/secretogranin) family. *Trends Biochem. Sci.* **16**, 27-30.
- Kaether, C. and Gerdes, H.-H. (1995). Visualization of protein transport along the secretory pathway using green fluorescent protein. *FEBS Lett.* **369**, 267-271.
- Kaether, C., Salm, T., Glombik, M., Almers, W. and Gerdes, H.-H. (1997). Targeting of green fluorescent protein to neuroendocrine secretory granules: a new tool for real time studies of regulated protein secretion. *Eur. J. Cell Biol.* **74**, 133-142.
- Kelly, R. B. (1993). Storage and release of neurotransmitters. *Cell* **72**, 43-53.
- Krömer, A., Glombik, M. M., Huttner, W. B. and Gerdes, H.-H. (1998). Essential role of the disulfide-bonded loop of chromogranin B for sorting to secretory granules is revealed by expression of a deletion mutant in the absence of endogenous granin synthesis. *J. Cell Biol.* **140**, 1331-1346.
- Lang, T., Wacker, I., Steyer, J., Kaether, C., Wunderlich, I., Soldati, T., Gerdes, H.-H. and Almers, W. (1997). Ca<sup>2+</sup>-triggered peptide secretion in single cells imaged with green fluorescent protein and evanescent-wave microscopy. *Neuron* **18**, 857-863.
- Lang, T., Wacker, I., Wunderlich, I., Rohrbach, A., Giese, G., Soldati, T. and Almers, W. (2000). Role of actin cortex in the subplasmalemmal transport of secretory granules in PC-12 cells. *Biophys. J.* **78**, 2863-2877.
- Lochner, J. E., Kingma, M., Kuhn, S., Meliza, C. D., Cutler, B. and Scalettar, B. A. (1998). Real-time imaging of the axonal transport of granules containing a tissue plasminogen activator/green fluorescent protein hybrid. *Mol. Biol. Cell* **9**, 2463-2476.
- Martelli, A. M., Baldini, G., Tabellini, G., Koticha, D. and Bareggi, R. (2000). Rab3A and Rab3D control the total granule number and the fraction of granules docked at the plasma membrane in PC12 cells. *Traffic* **1**, 976-986.
- Mercer, J. A., Seperack, P. K., Strobel, M. C., Copeland, N. G. and Jenkins, N. A. (1991). Novel myosin heavy chain encoded by murine dilute coat colour locus [published erratum appears in *Nature* 1991 Aug 8; 352(6335):547]. *Nature* **349**, 709-713.
- Mermall, V., Post, P. and Mooseker, M. (1998). Unconventional myosins in cell movement, membrane traffic, and signal transduction. *Science* **279**, 527-533.
- Nakata, T., and Hirokawa, N. (1992). Organization of cortical cytoskeleton of cultured chromaffin cells and involvement in secretion as revealed by quick-freeze, deep-etching, and double-label immunoelectron microscopy. *J. Neurosci.* **12**, 2186-2197.
- Ohashi, M. and Huttner, W. B. (1994). An elevation of cytosolic protein phosphorylation modulates trimeric G-protein regulation of secretory vesicle formation from the trans-Golgi network. *J. Biol. Chem.* **269**, 24897-24905.
- Ong, L. L., Lim, A. P., Er, C. P., Kuznetsov, S. A. and Yu, H. (2000). Kinectin-kinesin binding domains and their effects on organelle motility. *J. Biol. Chem.* **275**, 32854-32860.
- Prekeris, R. and Terrian, D. M. (1997). Brain myosin V is a synaptic vesicle-associated motor protein: evidence for a Ca<sup>2+</sup>-dependent interaction with the synaptobrevin-synaptophysin complex. *J. Cell Biol.* **137**, 1589-1601.
- Rapp, S., Saffrich, R., Anton, M., Jäkke, U., Ansorge, W., Gorgas, K. and Just, W. W. (1996). Microtubule-based peroxisome movement. *J. Cell Sci.* **109**, 837-849.
- Reck-Peterson, S. L., Provance, D. W., Jr., Mooseker, M. S. and Mercer, J. A. (2000). Class V myosins. *Biochim. Biophys. Acta.* **1496**, 36-51.
- Rogers, S. L. and Gelfand, V. I. (1998). Myosin cooperates with microtubule motors during organelle transport in melanophores. *Curr. Biol.* **8**, 161-164.
- Rudolf, R., Salm, T., Rustom, A. and Gerdes, H.-H. (2001). Dynamics of immature secretory granules: role of cytoskeletal elements during transport, cortical restriction and F-actin-dependent tethering. *Mol. Biol. Cell.* **12**, 1353-1365.
- Schliwa, M. (1999). Molecular motors join forces. *Nature* **397**, 204-205.
- Tabb, J. S., Molyneaux, B. J., Cohen, D. L., Kuznetsov, S. A. and Langford, G. M. (1998). Transport of ER vesicles on actin filaments in neurons by myosin V. *J. Cell Sci.* **111**, 3221-3234.
- Tai, A. W., Chuang, J. Z., Bode, C., Wolfrum, U. and Sung, C. H. (1999). Rhodopsin's carboxy-terminal cytoplasmic tail acts as a membrane receptor for cytoplasmic dynein by binding to the dynein light chain Tctex-1. *Cell* **97**, 877-887.
- Tooze, S. A., Flatmark, T., Tooze, J. and Huttner, W. B. (1991). Characterization of the immature secretory granule, an intermediate in granule biogenesis. *J. Cell Biol.* **115**, 1491-1503.
- Tvaruskó, W., Bentele, M., Misteli, T., Rudolf, R., Kaether, C., Spector, D. L., Gerdes, H.-H. and Eils, R. (1999). Time-resolved analysis and visualization of dynamic processes in living cells. *Proc. Natl. Acad. Sci. USA* **96**, 7950-7955.
- Vallee, R. B. and Sheetz, M. P. (1996). Targeting of motor proteins. *Science* **271**, 1539-1544.
- Wang, F. S., Wolenski, J. S., Cheney, R. E., Mooseker, M. S. and Jay, D. G. (1996). Function of myosin-V in filopodial extension of neuronal growth cones. *Science* **273**, 660-663.
- Wang, F., Chen, L., Arcucci, O., Harvey, E. V., Bowers, B., Xu, Y., Hammer, J. A., 3rd and Sellers, J. R. (2000). Effect of ADP and ionic strength on the kinetic and motile properties of recombinant mouse myosin V. *J. Biol. Chem.* **275**, 4329-4335.
- Wu, X., Bowers, B., Wei, Q., Kocher, B. and Hammer, J. A., 3rd (1997). Myosin V associates with melanosomes in mouse melanocytes: evidence that myosin V is an organelle motor. *J. Cell Sci.* **110**, 847-859.
- Wu, X., Bowers, B., Rao, K., Wei, Q. and Hammer, J. A., 3rd (1998). Visualization of melanosome dynamics within wild-type and dilute melanocytes suggests a paradigm for myosin V function In vivo. *J. Cell Biol.* **143**, 1899-1918.
- Wu, X., Rao, K., Bowers, M. B., Copeland, N. G., Jenkins, N. A. and Hammer, J. A., 3rd (2001). Rab27a enables myosin Va-dependent melanosome capture by recruiting the myosin to the organelle. *J. Cell Sci.* **114**, 1091-1100.